Available online at www.sciencedirect.com

ScienceDirect

Procedia CIRP 79 (2019) 180–185

www.elsevier.com/locate/procedia

12th CIRP Conference on Intelligent Computation in Manufacturing Engineering, 18-20 July 2018, Gulf of Naples, Italy

A vibration control for disassembly of turbine blades

Santiago D. Mullo[a], Edwin Pruna[a], Julius Wolff[b,*], Annika Raatz[b]

[a]*Universidad de las Fuerzas Armadas ESPE, Sangolqui, Ecuador*
[b]*Institute of Assembly Technology, An der Universität 2, Leibniz Universität Hannover, 30823 Garbsen, Germany*

* Corresponding author. Tel.: +49-(0)511-762-18248; fax: +49-(0)511-762-18251. *E-mail address:* wolff@match.uni-hannover.de

Abstract

Typically, disassembly forces are unknown due to high forces or high temperatures during product operation, where assembly connections solidify. For the regulation of disassembly forces a controller is developed. The controller is formed for two steps: The first step is a PID controller that produces a force, which overcomes a solidifying force slightly. The second step is a vibration controller with a FM modulation to regulate the frequency of impacts. Vibrations are useful for decreasing the force amplitude for caring the joined components. Finally, the control is validated with disturbances in a simulation.

Peer-review under responsibility of the scientific committee of the 12th CIRP Conference on Intelligent Computation in Manufacturing Engineering.

Keywords: Disassembly; Force control; Friction model; Vibration control

1. Introduction

Many industries such as the aviation industry consume scare resources generating pollution that affects the entire product life cycle from raw material to its final disposal producing high environmental loads. The life cycle of a product begins with the extraction of the raw material. This is followed by the manufacturing and assembly phase. After the production phase, the use phase starts, where some products go through a maintenance or repair phase or the materials are recycled [1].

Some of the materials of aircraft components are costly to produce, since they are made of materials such as composites and alloys with very high mechanical strength and resistance to high temperatures and corrosion [2]. These parts, like turbine blades are subjected to rapid heating and cooling during and after a flight, which causes stress and wear on the components. With regard to this publication, a solidification in its assembly connections –the connection to the disc- is generated.

Nowadays, objectives such as components reuse, remanufacture and recycling of components constitute some important reasons for the product disassembly. Nevertheless, industrial wastes, for example in the automotive industry, are often simply scrapped (dismantling, shredding and sorting) because it is currently too expensive to recover them [3]. However, there are few partially automated cases such as disassembly of electronics components [4]. The disassembly process is worthwhile if the products contains valuable material such as gold or the components have a high value such as parts of trains, aircrafts, and windmills [5].

Disassembly is formally defined as the systematic separation of components and can be categorized into several types, such as destructive or non-destructive and partial (selective) or complete (full) disassembly [6]. The choice of separation procedures dependents mainly on the types of connections between the components. Easy to disassembly are screwing or joined connection in contrast to welded or casted components (filling, inserting) that require complex or simply separation operations, respectively. Generally, a non-destructive disassembly technology is only possible, if a product has the required assembly connections. Nevertheless, these connections can solidify, making it a challenge to realize a non-destructive process.

Due to the fact that the solidification state and resulting internal forces in the assembly connections are unknown, disassembly processes are usually performed manually [7]. For an automatic tool control, this means that disassembly forces

2212-8271
Peer-review under responsibility of the scientific committee of the 12th CIRP Conference on Intelligent Computation in Manufacturing Engineering.
10.1016/j.procir.2019.02.041

adapt in the process. For this purpose, a control system is built up and a variance-based friction model is created for testing the control. The variances of the reaction forces represent the undetermined solidification forces.

Force vibrations are used to avoid jamming of the joining partners and to get an efficient energy input into the components, which is the advantage of force vibrations. Thus, force amounts can be reduced and be exploited for a component-friendly disassembly.

2. Related Work

A process of solidification can have various causes. In a turbine, hot gas corrosion and adhesion are major wear mechanisms. Hot gas corrosion is caused by components of the fuel and the air (e.g. sea salt) flowing through the engine and produces solidifications in the contact surfaces of a connection. Surface corrosion can increase the loosening torque of a screw, for example, up to 45% [8]. Adhesion in contrast is caused by molecular interactions on the boundary surfaces of the assembly connection. Deformations of roughness peaks and the separation of material fragments can increase the adhesion forces [9]. Besides the solidification caused by separated particles of the connection itself, foreign particles like sand can cause additional blockades in the connection. These many influences and their interaction make the determination of the disassembly force very difficult, so that the force is adjusted in the process by a control system. Therefore, a correct model is essential for the design of force controllers. In this work, the LuGre friction model is applied to reproduce the characteristics of the disassembly process, where the friction represents the solidification and a random value the unknown state. In this work, a PID controller is used in order to get a disassembly force, which can handle these deviations.

PID controllers are widely used in many industrial processes and recently in other fields such as for the control and damp of the vibrations generated in smart structures. One solution has been the implementation of an active vibration control based on PID algorithm and using the piezoelectric bounded smart structures [10]. However, finding the right control gains is important to satisfying and robust performance.

The force amplitude should be kept as low as possible for a disassembly process that is gentle on components and actuator-friendly. In order to avoid slowing down the process, the impact frequencies are to be increased [11].

3. Friction Model

Although materials with high mechanical strength and corrosion resistance are used in the aircraft engine, due to the operational loads it has to withstand. The assembly connections between the parts and the degree of solidification strongly define the disassembly characteristics of the turbine blades.

Therefore, the reaction force during the disassembly process, a solidifying force *R,* is completely unknown and is modeled by the friction between the joined partners.

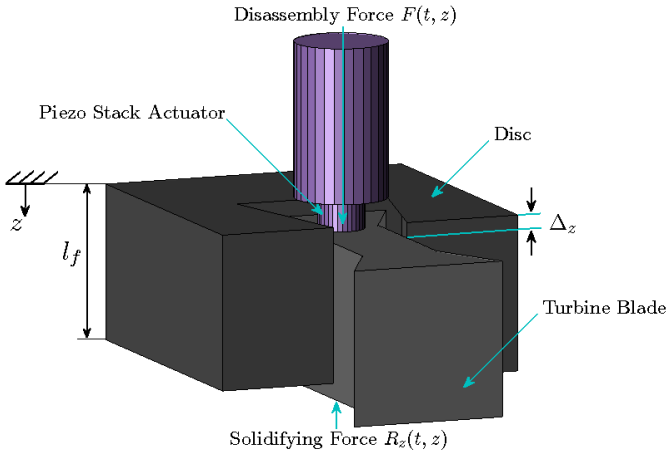

Fig. 1. Simplified model of disassembly task.

The reaction force has to be succeeded by a disassembly force, in order to get a movement.

Figure 1 shows the development of this process. A piezo actuator applies the disassembly force *F(t,z).* The actuator causes the displacement of the turbine blade position *z(t)* in the disc. If the distance *Δz* is smaller, then the turbine blade will have less risk of damage because of lower forces.

A solidification behavior is described by a friction model with a random force variance. Friction opposes motion and is created by microscopic imperfections and irregularities of two surfaces in contact with each other. Further, it is present in mechanical systems that involve parts in contact. These characteristics are important for establishing the estimation of solidification behavior. The LuGre model is an efficient friction model that contains all the features in regions I, II and III (Figure 2b) that correspond to static, transient and dynamic cases respectively. Figure 2b shows these regions, region II is the most complicated to model. In this region starts the relative movement of the assembled components and thus the disassembly process begins.

When the contact of two surfaces at microscopic level is visualized, irregularities due to the presence of roughness are observed. The LuGre model proposes to describe it as when two rigid bodies come into contact through elastic bristles [12] (Fig. 3). The behavior is described by:

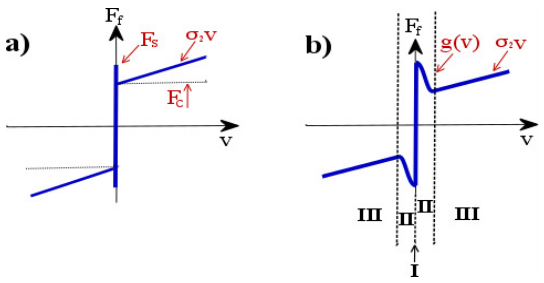

Fig. 2. Representation of friction behavior with its regions (a) Coulomb Friction F_C, Stiction Friction F_S and viscous friction σ_2; (b) LuGre model with Stribeck curve.

$$F_f = k_e \cdot z + c \cdot \frac{dz}{dt} \tag{1}$$

$$\frac{dz}{dt} = v - \frac{|v|}{g(v)} \cdot z \tag{2}$$

$$g(v) = F_C + (F_S - F_C) \cdot e^{-\left(\frac{v}{v_S}\right)^2} \tag{3}$$

Where F_f is the friction, k_e is stiffness of the bristles, c is damping of the bristles, v is the relative velocity between the two bodies, z is the average deflection of bristles, F_c is the coulomb force, F_s is the stiction force (break-away friction) and v_s is the velocity of Stribeck. For constant velocities, the steady-state friction is indicated by F_{SS} associated with velocity and the coefficient of viscous friction σ_2 is given by

$$F_{SS} = g(v) \cdot sgn(v) + \sigma_2 \cdot v$$

$$= \left[F_C + (F_S - F_C) \cdot e^{-\left(\frac{v}{v_S}\right)^2}\right] \cdot sgn(v) + \sigma_2 \cdot v \tag{4}$$

Figure 3b shows the average deflection of the bristles for region I (compare Figure 2b). If the force applied does not exceed the stiction force, the reaction force is defined by region I. The turbine blade will begin to slide, if the force applied exceeds the stiction force F_s. It will begin to enter region II and consequently region III. These regions show that the bristles become over-deflected generating disassembly motion, and the random behavior of this phenomenon is captured by the behavior of the bristles [12]. For this research, it is necessary to modify certain parameters of the LuGre friction model. The contact surface during disassembly of the turbine blade decreases from a maximum value until the completion of the disassembly. With progressing disassembly, the coulomb force F_C and the stiction force F_s will be smaller and will depend on the position of the blade $z(t)$.

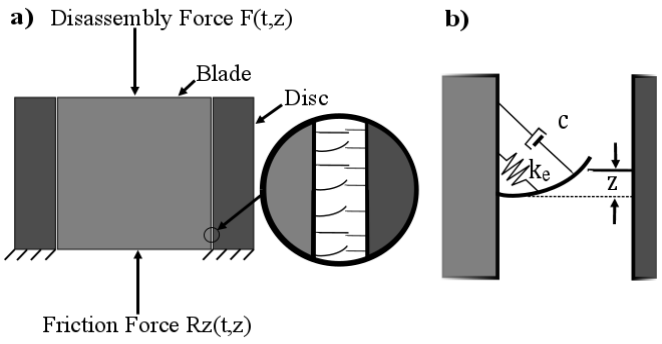

Fig. 3. Microscopic behaviour of the LuGre friction model (a) Bristles to describe the solidification; (b) Average deflection of the bristles.

Table 1. Parameters for Simulation of the Lugre Friction Model.

Name	Symbol	Value	Unit
Initial stiction friction	F_{SO}	450	$[N]$
Initial coulomb friction	F_{CO}	360	$[N]$
Stiffness coefficient	k_e	30000000	$[N/m]$
Damping coefficient	c	$1,6 \cdot k_e$	$[N \cdot s/m]$
Stribeck velocity	v_S	0.09	$[m/s^2]$
Total disassembly distance	l_f	0.1	$[m]$
Mass	m	1	$[kg]$

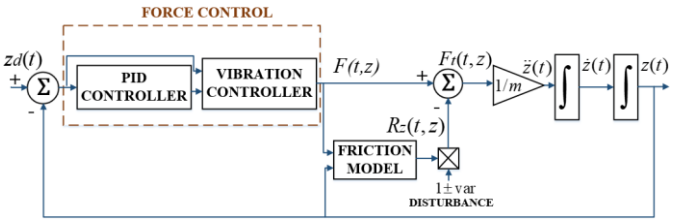

Fig. 4. Block Diagram of Control System.

F_{SO} and F_{CO} represent the initial values of the stiction and coulomb forces respectively and m is the mass of the turbine blade. Therefore, equations (1) and (4) are modified for the estimation of the solidification by equations (5) and (6), due to the speed of the system, the viscous friction not is considered.

$$R_Z(t,z) = k_e \cdot z(t) + c \cdot \frac{dz(t)}{dt} \tag{5}$$

$$R_Z(t,z) = \left[F_C(z) + (F_S(z) - F_C(z)) \cdot e^{-\left(\frac{v}{v_S}\right)^2}\right] \cdot sgn(v) \tag{6}$$

The parameters chosen for the simulation have been multiplied and modified slightly with a high gain compared to those proposed by [13]. These are defined by table 1.

The friction force of the LuGre model does not represent the real course of the solidifying force. To get a similar effect with a varying unknown process force, the friction force is multiplied by a random number *1+/-var* creating a disturbance defined for the variable *var*. The friction force can take any value from *(1-var)Rz(z)* to *(1-var)Rz(z)*.

Figure 4 shows the system block diagram. To obtain the position of the displacement *z(t)*, the second Newtonian law applies to the relative force $F_t(t,z)$.

4. Force Controller Design

The design of the controller is based on pole analysis of the closed loop system transfer function. Therefore, it is necessary to reduce the block diagram. Although the Stribeck curve gives a perspective of the transition between static friction and dynamic friction rather than a discontinuous fall, to facilitate the work of the control design, it is necessary to eliminate this effect and use the equation (7). The upper formula is used for

the calculation of R_Z in the case of stiction (Figure 2a), while the bottom formula is used for sliding friction. Figure 2a shows the friction behaviour for the controller design.

$$R_z(t,z) = \begin{cases} k_e \cdot z(t) + c \cdot \dfrac{dz}{dt} & if\ F(t,z) \le F_S(z) \\ F_C(z) & if\ F(t,z) > F_S(z) \end{cases} \quad (7)$$

4.1. PID controller design

For the calculation of the PID controller gains, only the regions I and III, defined for equation (7) corresponding to static and dynamic friction cases respectively, are taken into account. The transfer function $T_S(s)$ for the static case is given by the following equation:

$$T_S(s) = \frac{\frac{kd_s}{m} \cdot s^2 + \frac{kp_s}{m} \cdot s + \frac{ki_s}{m}}{s^3 + \left(\frac{c + kd_s}{m}\right) \cdot s^2 + \left(\frac{k_e + kp_s}{m}\right) \cdot s + \frac{ki_s}{m}} \quad (8)$$

kp_s , kd_s and ki_s are the proportional, derivative and integral gains respectively for the static case.

To reduce the level of complexity of third order system, it is compared with a stable second order system multiplied by a pole located in a stable zone given by equation (9).

$$P(s) = (s + a) \cdot (s^2 + 2 \cdot \varepsilon \cdot \omega \cdot s + \omega^2) \quad (9)$$

In this equation (11) a is the pole in stable zone, ω is the natural frequency of the system and ε is the damping coefficient of the system. Equalizing the equations (8) with (9), the tuning constants are obtained:

$$kp_s = (\omega^2 + 2 \cdot a \cdot \varepsilon \cdot \omega) \cdot m - k_e \quad (10)$$

$$kd_s = (2 \cdot \varepsilon \cdot \omega + a) \cdot m - c \quad (11)$$

$$ki_s = a \cdot \omega^2 \cdot m \quad (12)$$

For the analysis in the dynamic case, an initial condition exists: The disassembly force $F(t,z)$ have already reached the stiction force and it will be equal to the coulomb force $F_{CO}(z)$. Here we assume that the force decreases proportionally. Since the inner forces of the assembly connections act in less contact area, which occurs proportionally with a change in length of the contact. The force $F_C(z)$ given by the equation (13).

$$F_C(z) = F_{C0}\left(1 - \frac{z}{l_F}\right) - mg \quad (13)$$

The transfer function $T_d(s)$ is given by:

$$T_d(s) = \frac{\frac{kd_d}{m} \cdot s^2 + \frac{kp_d}{m} \cdot s + \frac{ki_d}{m}}{s^3 + \left(\frac{kd_d}{m}\right) \cdot s^2 + \left(\frac{1 + kp_d}{m}\right) \cdot s + \frac{ki_d}{m}} \quad (14)$$

In this equation kd_d and ki_d are the proportional, derivative and integral gains respectively for the dynamic case. In a situation similar to that of the static case when equations (9) and (14) are equalized, the tuning constants are given by:

$$kp_d = (\omega^2 + 2 \cdot a \cdot \varepsilon \cdot \omega) \cdot m - 1 \quad (15)$$

$$kd_d = (2 \cdot \varepsilon \cdot \omega + a) \cdot m \quad (16)$$

$$ki_d = a \cdot \omega^2 \cdot m \quad (17)$$

The control parameter ε and ω for static and dynamic cases are defined for a quick process, the location of the introduced pole is in $a=200$, and to obtain ω is necessary to consider the settling time at 2% given by $t_S=0{,}0005s$ and $\varepsilon=1$. The response velocity causes the control actions (disassembly force) to remain close to the coulomb force, for which it is necessary to pay attention to dynamic gains, then the final tuning gains are given by:

$$kp_t = 0.1 \cdot kp_s + 0.9 \cdot kp_d \quad (18)$$

$$kd_t = 0.1 \cdot kd_s + 0.9 \cdot kd_d \quad (19)$$

$$ki_t = 0.1 \cdot ki_s + 0.9 \cdot ki_d \quad (20)$$

4.2. Vibration controller design

To work with vibration it is necessary to modify the control parameters $\varepsilon=1$ and $t_S=0{,}0005s$ for obtaining a gentler response. Moreover, vibration control uses the FM modulation principle, where the input amplitude is that of the PID controller output and the modulation parameter is the error (compare figure 5).

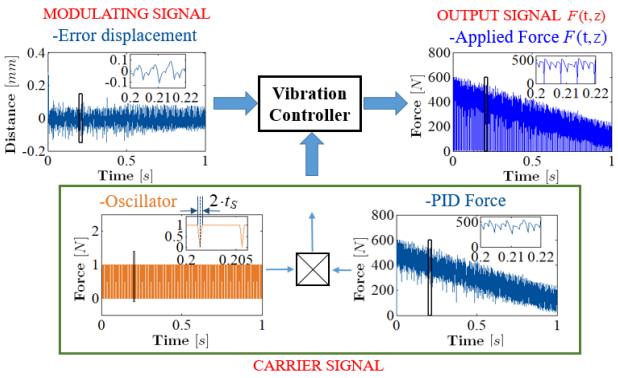

Fig. 5. Vibration controller based in FM modulation.

The output frequency will be proportional to the amount of error, furthermore to reduce even more amplitude the pulse-width below is the least possible. In addition, in the simulation it is essential to be careful with aliasing phenomena and apply the Nyquist criterion to establish model frequency, sampling frequency, vibration frequency range, etc. This is why the control frequency ranges from 80[Hz] to 160[Hz].

5. Results

The table 2 shows the PID controller gains (x1000) for the implementation of the force controller with and without vibration, where in both cases the dynamic ratio (factor 0.9) prevails over the static ratio (factor 0.1), as seen in equation (14). The integral gains are very high, which results in a quick response of the control.

5.1. Force control

Figure 6 shows the solidifying force *Rz(t,z)* with a disturbance range of ±5% when applying a force control *F(t,z)*. It can be seen, that the disassembly force recurrently exceeds the solidifying force by 200 N, which is necessary to overcome the static friction and the inertia of the disassembly object. Once the disassembly object starts moving, dynamic friction occurs and the solidifying forces declines. Subsequently, the disassembly Force also declines until the movement stops. This behaviour is comparable to the stick-slip-effect.

Table 2. PID control gains (x1000)

Description	Control without Vibration			Control with Vibration		
	Static	Dynamic	Total	Static	Dynamic	Total
Proportional Gain	31200	19,2	3137,3	8168,3	12,6	828,2
Derivative Gain	7,2000	0,0046	0,7242	6,5846	0,0044	0,6625
Integral Gain	12800000	3655	1283289	8218277	2347	823940

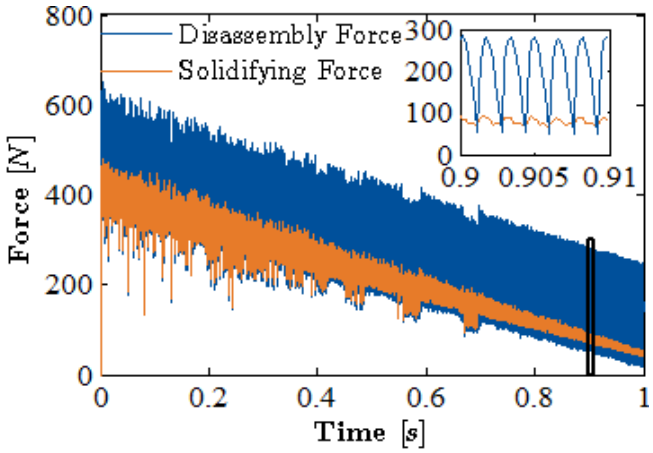

Fig. 6. Control and Solidifying Forces with disturbance range of±5%.

5.2. Force control with vibration

Figure 7 shows the solidifying force $R_z(t,z)$ with a disturbance range of ±5% when applying a force control with vibration $F(t,z)$. The vibrations create a forced stick-slip-movement. The disassembly force exceeds the solidifying force by only 150 N (compared to 200 N without vibrations). This confirms the assumption, that vibrations can reduce the necessary disassembly force.

Figure 8 shows the final results of the two controllers. The force applied with vibration is smoother than the force applied without vibration. This is due to the forced stick-slip-movement of the disassembly object.

Figure 9 shows the errors defined by the absolute error integral (IAE) that is used for performance comparison to present results in each interaction with different variation ranges until before the controller allows an unstable response. For the control without vibration its maximum disturbance range is ±8.5% while for the vibration control its range is ±12.5%. That means that by using vibrations, the operating range of the controller can be extended, whereby higher variations of the solidifying force can be tolerated, which enhances the reliability of the disassembly system.

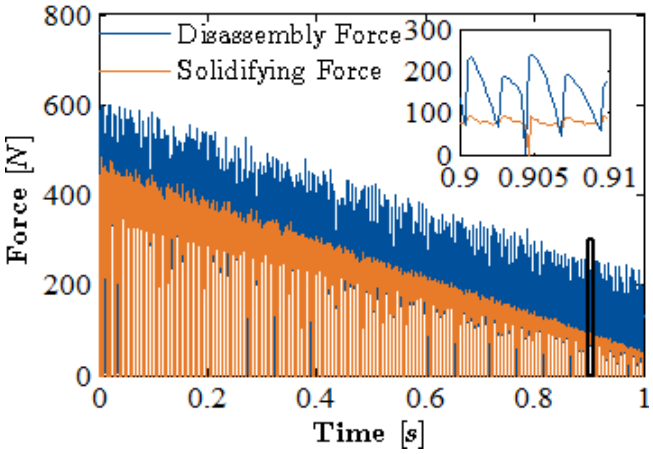

Fig. 7. Vibration Control and Solidifying Force with disturbance range of±5%.

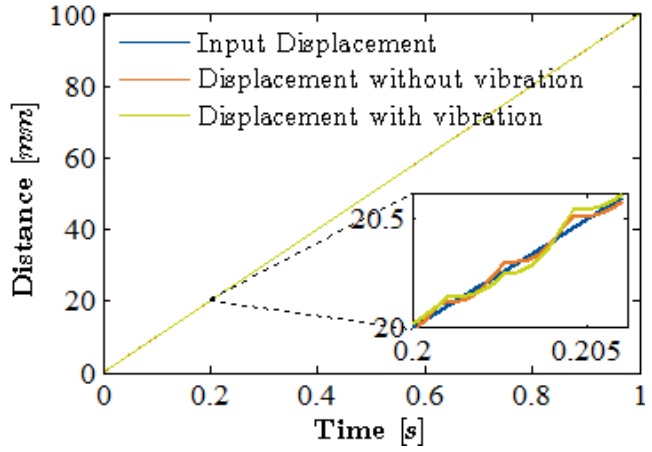

Fig. 8. Desired and Measured Displacements with and without Vibration Control.

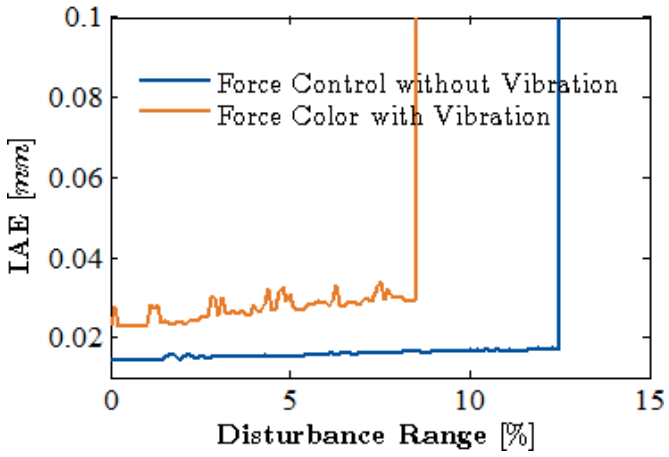

Fig. 9. Error results of the force controller with and without vibration and disturbance ranges

6. Conclusion

Solidification is an undesired phenomenon in disassembly that is present in joined components due to the operation, causing difficulty in knowing the reaction force. Therefore for the development of an automated disassembly system is difficult, because the solidification has to be estimated beforehand.

In this work The solidifying force was calculated with the LuGre friction model and was used for the development a PID force and a vibration controller. The first was implemented to apply a correct disassembly force with the calculation of its gains tuning based on the poles analysis of static and dynamic cases. Further the control parameters were designed to obtain a quick response and the desired displacement, creating a high quality disassembly process. Furthermore, strain of the disassembly object and wear on the piezo actuator were reduced by decreasing the applied force amplitude with the implementation of vibrations control based on FM modulation.

Disturbance is an unwanted effect that affects the process operation. In this work, disturbance in solidifying force was introduced. to compensate the estimation error regarding the real disassembly. Several tests have been introduced with different disturbance values that have been progressively increased and analyzed with the Integral Absolut Error (IAE). Finally, the simulation is implemented with Simulink/MATLAB using the Simmechanics toolbox, obtaining excellent results up to a maximum acceptable disturbance range.

Acknowledgments

The authors kindly thank the German Research Foundation (DFG) for the financial support to accomplish the research project A5 "Adaptable and Component-Protecting Disassembly in the Regeneration Path" within the Collaborative Research Center (CRC) 871 - Regeneration of Complex Capital Goods.

7. References

[1] Duflou JR, Seliger G, Kara S, Umeda Y, Ometto A, Willems B. Efficiency and feasibility of product disassembly. A case-based study. In CIRP Annals, Volume 57, Issue 2, 2008, Pages 583-600.
[2] Asmatulu E, Overcash M, Twomey J. Recycling of Aircraft. State of the Art in 2011. Journal of Industrial Engineering, vol. 2013, Article ID 960581, 2013, 8 pages.
[3] Tasala K, Luttropp C, Björklund A. Investigating improved vehicle dismantling and fragmentation technology. Journal of Cleaner Production, Volume 54, 2013, Pages 23-29.
[4] Merdan M, Lepuschitz W, Meurer T, Vincze M. Towards ontology-based automated disassembly systems. IECON 2010 - 36th Annual Conference on IEEE Industrial Electronics Society 2010, pp. 1392-1397.
[5] Åkermark AM. Design for Disassembly and Recycling. In: Krause FL., Seliger G. (eds) Life Cycle Networks. Springer, Boston, MA. 1997.
[6] Chang MML, Ong SK, Nee AYC. Approaches and Challenges in Product Disassembly Planning for Sustainability, In Procedia CIRP, Volume 60, 2017, Pages 506-511.
[7] Desai A, Mital A. Evaluation of disassemblability to enable design for disassembly in mass production, In International Journal of Industrial Ergonomics, Volume 32, Issue 4, 2003.
[8] Kahmeyer M. Flexible Demontage mit dem Industrieroboter am Beispiel von Fernsprech-Endgeräten, Faculty of Engineering Design and Production Engineering, Stuttgart, Springer-Verlag, 1995, pp 50-60.
[9] Ahgary A. Eine Analyse der Verschleißmechanismen in der Anwendung der Hüftgelenkendoprothetik, Berlin, diplom.de, 2002.
[10] Zhang S, Schmidt R, Qin X. Active vibration control of piezoelectric bonded smart structures using PID algorithm, In Chinese Journal of Aeronautics, Volume 28, Issue 1, 2015, Pages 305-313.
[11] Wolff J, Yan M, Schultz M, Raatz A. Reduction of Disassembly Forces for Detaching Components with Solidified Assembly Connections, In Procedia CIRP, Volume 44, 2016, Pages 328-333.
[12] Canudas de Wit C, Olsson H, Astrom KJ and Lischinsky P. A new model for control of systems with friction in IEEE Transactions on Automatic Control, vol. 40, no. 3, pp. 419-425, Mar 1995.
[13] Johanastrom K, Canudas-de-Wit C. Revisiting the LuGre friction model, in IEEE Control Systems, vol. 28, no. 6, pp. 101-114, Dec. 2008.